Progress In Electromagnetics Research C, Vol. 125, 117–131, 2022

A Miniaturized Circularly Polarized Multiband Antenna for Wi-Max, C-Band & X-Band Applications

Sonali Kumari[1, *], Yogendra K. Awasthi[1], and Dipali Bansal[2]

Abstract—In this paper, a compact triangular-shaped multiband antenna is proposed for linear as well as circular polarization. The proposed antenna is well suitable for Wi-Max, C-band, and X-band applications. 2.4 GHz is very well suitable for RFID applications. The antenna is excited with a feed of variable width at one corner of the main patch. The parametric analysis has been done for feed width, slot cutting on the ground, and tapering cut at both remaining corners of the main patch. Circular polarization is achieved due to a tapering cut. It achieved circular polarization at 2.4 and 9.8 GHz and linear polarization at 4.31 and 6.75 GHz. The structure shows an impedance bandwidth of 2.13–3.02 GHz and 4.01–10.00 GHz. The measured peak gain is achieved to be 3.66 dB. A good agreement is found between simulated and experimental results.

1. INTRODUCTION

In the last decade, the demand for compact, portable multiband antenna has increased due to the increased demand for wireless applications. In the case of multiband operation, a single antenna can be used for various applications. At a time, one part of the antenna is used for one band of frequency, while other parts are used for another band of frequency. Till now, various kinds of work have been done on achieving multibands. Slot cutting, defected ground plane, use of metamaterial, and fractal methods have been different ways to achieve multibands [1–6].

In multiband operation, circularly polarized (CP) antennas are more useful than linearly polarized (LP) antennas in the case of WLAN/Wi-Max, radiofrequency identification (RFID), mobile communication, and satellite communication as in such cases, the orientations of the transmitting and receiving antennas are not important. CP antenna can reduce Faraday's rotation effect in the ionosphere, and multipath interference is also less. So in this case there is less chance of polarization mismatches, hence it is well suitable for communication devices [7, 8].

A lot of techniques have been reported in the past to achieve a multiband CP antenna. Every technique has its advantages as well as some disadvantages. Various types of slit in patches have been used to design CP antennas [9–13]. However, this is suitable for 2–4 GHz frequency range only. The authors in [14] suggested a technique to achieve multiband CP by cutting the corner of two parasitic elements. However in this case, bandwidth is less. One more multiband CP has been developed by the authors in [15] using truncated corners. Further, asymmetric slots and annular slots are other methods for achieving CP [16, 17]. An L-shaped slit has been used to design a CP antenna. This antenna has been proposed for C and X band applications [18], but it has a limitation of large size. With the use of defected ground structure (DGS), broadband can be achieved in a CP antenna [19–21]. Split ring resonator [22], C-shaped array [23], C-shaped split ring [24, 25], triangle-shaped antenna with tuning

Received 25 August 2022, Accepted 3 October 2022, Scheduled 9 October 2022

* Corresponding author: Sonali Kumari (sinha.sonali08@gmail.com).

[1] Manav Rachna International Institute of Research and Studies University, Faridabad, India. [2] G.B. Pant, DSEU, Okhla 1 Campus, New Delhi, India.

stub [26], and monopole antenna with loops [27] are some other methods to achieve CP antenna. F-shaped antenna with a DGS [28] and hexagon-shaped antenna with a DGS [29] have also been used to achieve CP antenna by the authors. One more multiband CP has been developed by the authors in [30] working on the compactness of design, but here bandwidth achieved is less.

Most of the papers discussed have either a large size antenna or narrow bandwidth. From the literature, it is clear that there is still a need to work towards smaller size, low profile circularly polarized multiband antenna. In this article, a compact truncated triangle-shaped circularly polarized multiband antenna has been proposed that is small in size $(35 \times 24 \times 1.6)\,\text{mm}^3$ and has multiple bands (2.13–3.02 GHz and 4.01–10.00 GHz). This antenna is well suitable for RFID, WLAN, C-band, and X-band applications. The proposed antenna is compact, and its fabrication is also easy and cheap, as it is designed on an easily available FR4 substrate. It also exhibits a 3-dB axial ratio at 2.4 GHz and 9.8 GHz.

The overview of the proposed antenna design is given in Section 2. It includes all the geometrical detail of the proposed design. Simulation and parametric analysis are discussed in Section 3 only. Section 4 includes the fabricated structure and experimental results. The conclusion is explained in Section 5.

2. PROPOSED ANTENNA DESIGN & GEOMETRY

The geometry of the proposed antenna is depicted in Figure 1. Initially, it consists of a simple triangular-shaped monopole antenna with microstrip feeding as shown in Figure 1. The relative permittivity and thickness of the substrate are 4.4 and 1.6 mm, respectively. The overall size of the antenna is $35 \times 24 \times 1.6\,\text{mm}^3$. The design and optimization of the antenna are carried out through HFSS v.13 software. Then to improve gain and enhancement of bandwidth, two rectangular slots $(13 \times 2)\,\text{mm}^2$ and $(11 \times 2)\,\text{mm}^2$ at the ground plane have been removed. In the 3rd step of the design, the tapered cut at the corner of the right side of the triangle has been removed. Then in the last step, one more triangle at the left corner of the patch has been removed. By tapered cut in the triangle, the antenna will become circularly polarized. It will become clearer through the axial ratio graph (to be discussed later on). The dimension of the tapering cut has been taken based on the parametric variation. All the values are given in Table 1. Figure 2 shows the geometry of the proposed design.

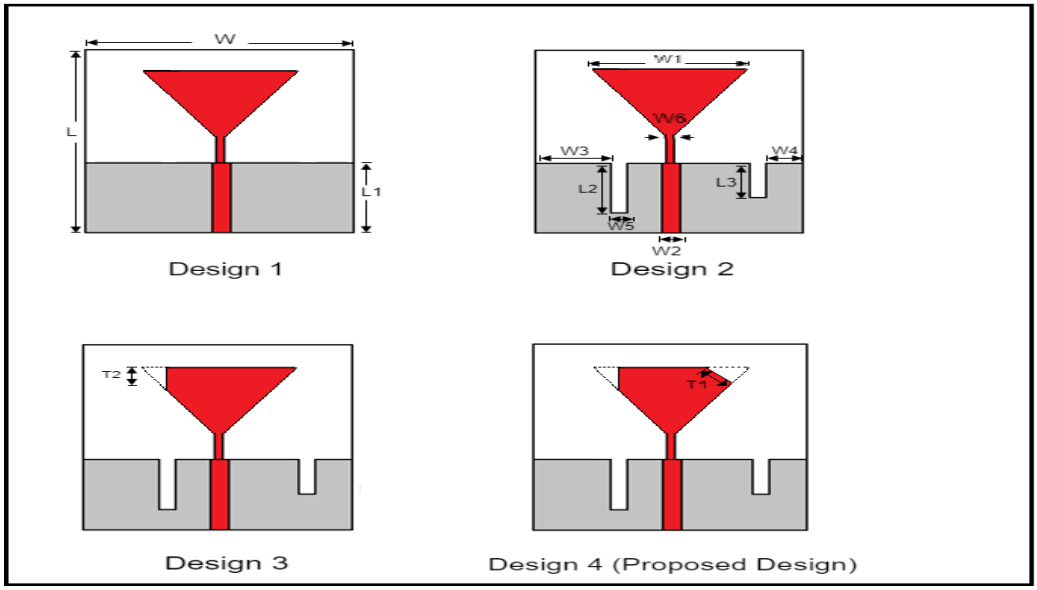

Figure 1. Evolution steps of the proposed antenna.

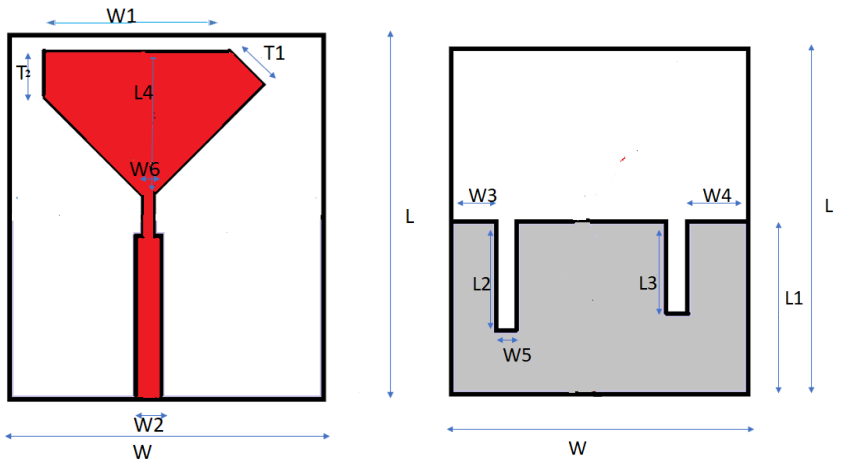

Figure 2. Geometry of the proposed antenna (Front side and back side).

Table 1. Key dimensions of proposed antenna.

Parameter	L	$L1$	$L2$	$L3$	$L4$	W	$W1$	$W2$	$W3$	$W4$	$W6$	$T1$	$T2$
Value (mm)	35	17.2	13	11	10	24	22	2	6	2.5	1	3	4

3. DISCUSSION ON SIMULATION AND PARAMETRIC VARIATION

3.1. Simulation Analysis

Figures 3(a) and 3(b) show simulated results of all the designs (given in Figure 1). Figure 3(a) is for return loss, Figure 3(b) for axial ratio, and Figure 3(c) for the gain plot. Initially, in design 1, the antenna resonates at 2.44 to 3.69 GHz bandwidth. At this stage, the gain is positive at 3.0 GHz to 3.4 GHz, but gain is still lower, and the maximum gain observed is 1.36 dB at 3.5 GHz. In design 2, the antenna resonates at 2.13 to 2.8 GHz bandwidth. Gain is positive at 2.19 to 2.56 GHz, while maximum gain is 1.85 dB at 2.25 GHz. In design 3, gain is positive at 4 to 8.87 GHz, and maximum gain is 2.66 dB at 5.37 GHz. Here the axial ratio is also less than 3 dB at 9.68 GHz. However, design 4 (i.e., proposed

Table 2. Comparison of design steps (From design 1 to proposed design).

Design Step	Frequency Band (GHz)	Maximum Reflection Coefficient (dB)	Corresponding resonant frequency (GHz)	Bandwidth (GHz)
Design 1	2.4–3.88	−24.17	3.01	1.48
Design 2	2.13–3.88 9.5–10	−18.07 −10.82	2.44 9.87	1.75 0.5
Design 3	2.13–2.94 4.06–7.37	−18.03 −20.47	2.50 4.31	0.81 3.31
Design 4 (Proposed Design)	2.19–2.94 4.06–10	−19.18 −26.53	2.56 9.81	0.75 5.94

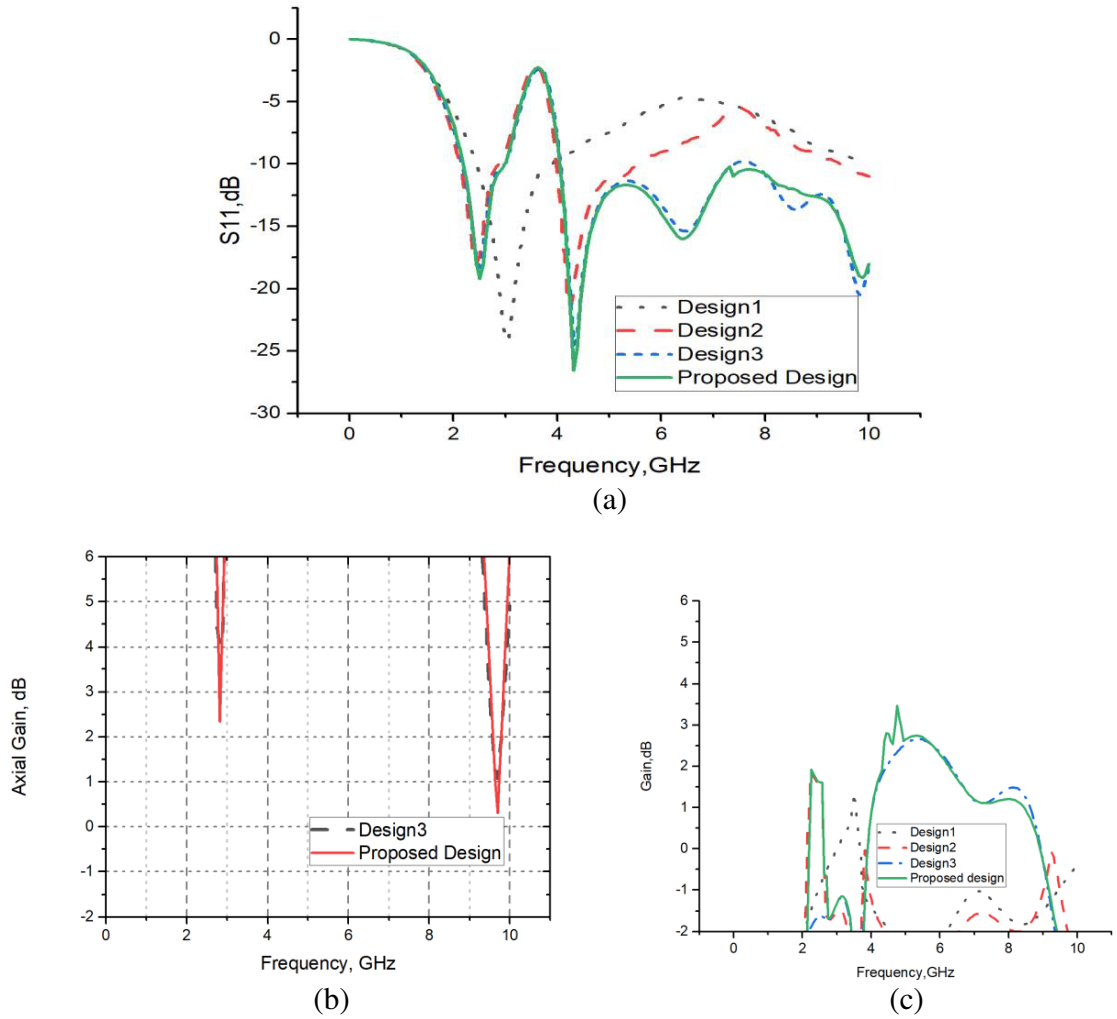

Figure 3. Simulation evolution steps of the proposed antenna; (a) return loss; (b) axial ratio; (c) gain vs frequency.

design) resonates at 2.19 to 2.94 GHz and 4.06 to 10 GHz, and the gain is also positive at 4 to 8.87 GHz. The maximum gain is 3.40 dB at 5.07 GHz. Here the axial ratio is less than 3 dB at 2.4 and 9.87 GHz. So at these two frequencies, the antenna is circularly polarized, and at the other resonant frequencies, it is linearly polarized which is clearer from the axial ratio graph given in Figure 3(b). At 2.4 GHz, axial ratio was observed at 2.2 dB, and at 9.8 GHz, axial ratio was observed at 0.2 dB. For circularly polarized antenna, the axial ratio should be below 3 dB. So the proposed design is circularly polarized at 2.4 GHz and 9.8 GHz, and it is linearly polarized at 4.5 GHz and 6.5 GHz. A comparison of S_{11} results is listed in Table 2.

3.2. Phenomenon of CP Development in Terms of Current Distribution

Figure 4 and Figure 5 show the illustration of CP. The simulated surface current distribution is shown at different time phases 0°, 90°, 180°, 270° for 2.4 GHz and 9.8 GHz. It is verified from Figure 4 and Figure 5 that the current magnitudes in 0° and 90° are similar to that in 180° and 270°, but the phases are opposite in direction. The total effect of current distribution is anticlockwise, and it can be referred to as left hand circularly polarized (LHCP) antenna.

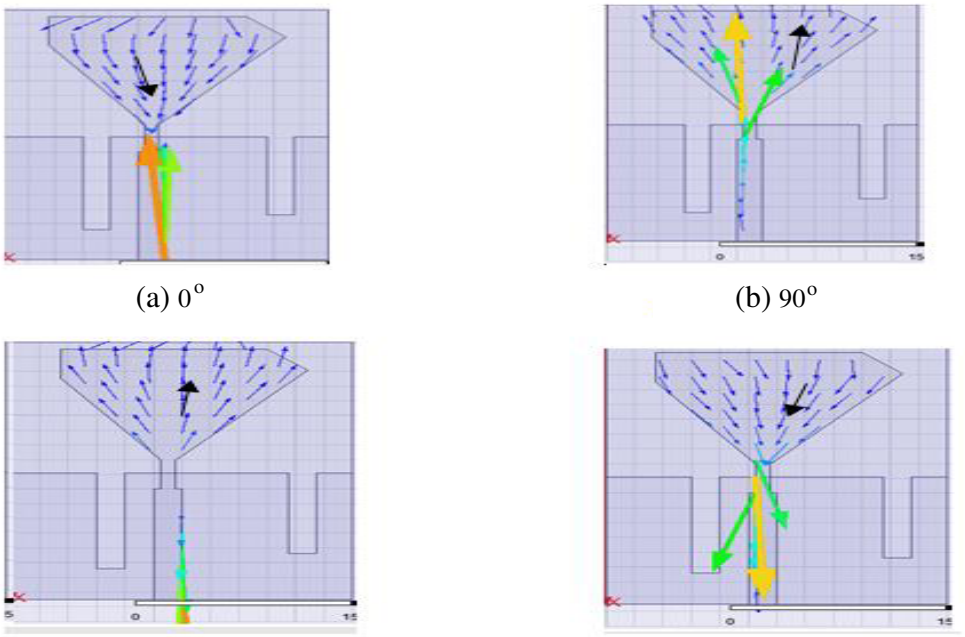

(a) 0° (b) 90°

(c) 180° (d) 270°

Figure 4. Simulated current distribution at 2.4 GHz: (a) 0°; (b) 90°; (c) 180°; (d) 270°.

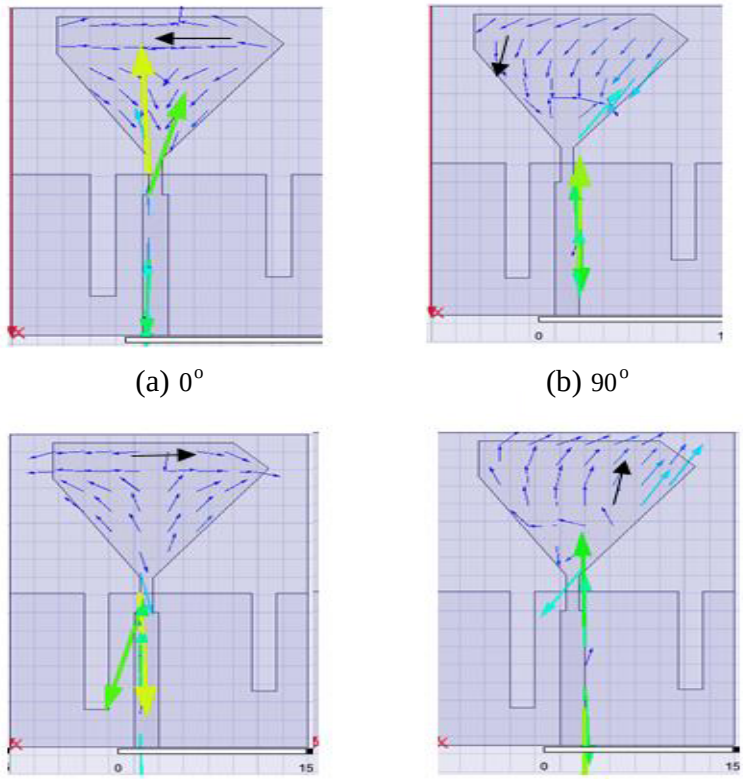

(a) 0° (b) 90°

(c) 180° (d) 270°

Figure 5. Simulated current distribution at 9.8 GHz: (a) 0°; (b) 90°; (c) 180°; (d) 270°.

3.3. Parametric Validation

A parametric variation is performed to validate the design performance. One parameter is varied while the others are kept unchanged to see the effect on the S_{11} parameter.

3.3.1. Parametric Change in Feed Width ($W2$)

In the proposed design, a modified feed line has been proposed, which is 1 mm at the joint of the patch, and it is 2 mm in width at the lower side. Figure 6 shows the parametric variation, where feed width is changed to uniform feed width of 1 mm and 2 mm, and the bandwidth is reduced. To improve bandwidth, modified feed width is proposed. It is clearer in Figure 6. The comparison in Table 3 gives a clearer idea about S_{11} due to parametric variation in $W2$.

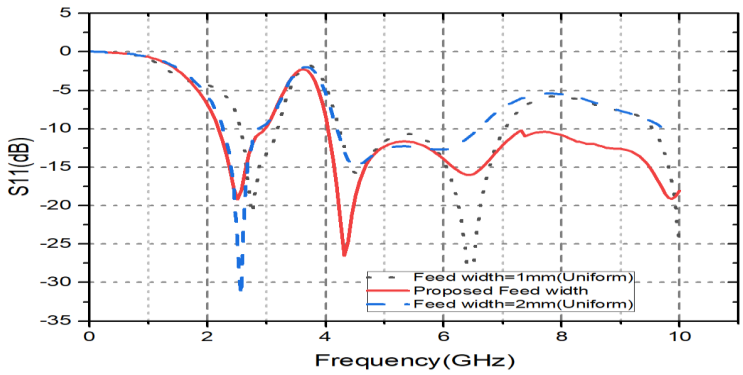

Figure 6. Simulated results of parametric change in feed width.

Table 3. Comparison of S_{11} results due to parametric variation of $W2$.

Feed Width W2 (mm)	Frequency Band (GHz)	Maximum Reflection coefficient (dB)	Resonating Frequency (GHz)	Bandwidth (GHz)
$W2 = 1$ (uniform)	2.56–3.13	−20.98	2.75	0.57
	4.25–7.01	−30.73	6.44	2.76
$W2$ = Variable (Proposed Design)	2.19–2.94	−19.18	2.50	0.75
	4.06–10	−26.53	4.31	5.94
$W2 = 2$ (uniform)	2.32–2.81	−31.60	2.56	0.49
	4.38–6.56	−14.92	4.50	2.18

3.3.2. Parametric Change in Slot Length at the Ground

Figure 7 shows parametric change in the slot length in the ground plane. The length of both rectangular slots ($L2$ and $L3$) is varied by 1 mm. In Figure 7(a), $L2$ slot length is varied while $L3$ remains the same. In Figure 7(b), $L3$ slot is varied while $L2$ remains the same. It is concluded that the S_{11} parameter and bandwidth are optimized in the proposed design. Table 4 and Table 5 give comparative idea of S_{11} due to parametric variation in $L2$ and $L3$, respectively.

3.3.3. Parametric Change in $T2$

The parametric change in the tapered cut of length $T2$ at the left corner of the patch is shown in Figure 8. From the patch, one small triangle from the left side corner is removed. Then the various

Table 4. Comparison of S_{11} result due to parametric variation of $L2$.

L2 (mm)	Frequency Band (GHz)	Maximum Reflection coefficient (dB)	Resonant Frequency (GHz)	Bandwidth (GHz)
$L2 = 12$	2.25–2.88 4.19–7.68	−18.45 −24.15	2.56 4.43	0.63 3.49
$L2 = 13$ (Proposed)	2.19–2.94 4.06–10	−19.18 −24.73	2.50 4.38	0.75 5.94
$L2 = 14$	2.19–2.94 4.06–10	−18.70 −24.09	2.50 4.25	0.75 5.94

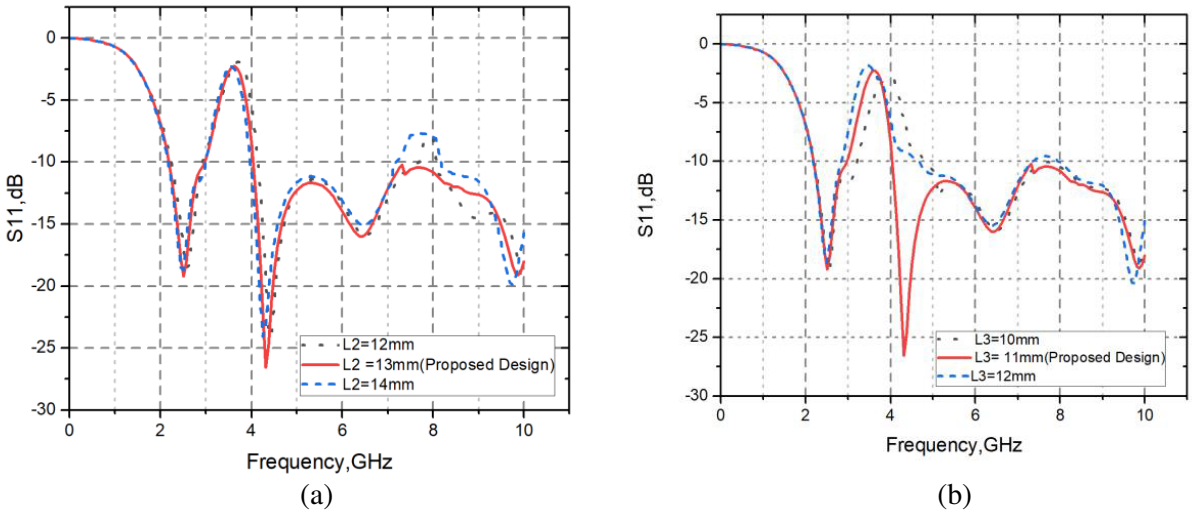

Figure 7. Simulated results of parametric change ground, (a) change in slot length $L2$, (b) change in slot length $L3$.

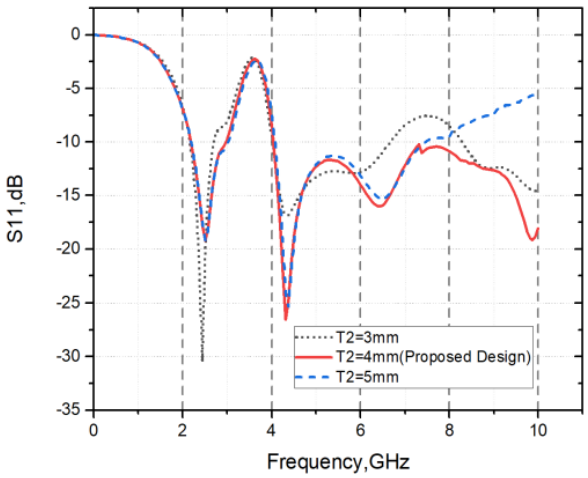

Figure 8. Simulation results of parametric change in $T2$.

Table 5. Comparison of S_{11} results due to parametric variation of $L3$.

L3 (mm)	Frequency Band (GHz)	Maximum Reflection Coefficient (dB)	Resonant Frequency (GHz)	Bandwidth (GHz)
$L3 = 10$	2.25–319	−19.48	2.56	0.94
	4.88–10	−18.58	9.87	5.12
$L3 = 11$ (Proposed)	2.19–2.94	−19.18	2.50	0.75
	4.06–10	−19.13	9.81	5.94
$L2 = 12$	2.19–2.81	−18.62	2.50	0.62
	4.69–10	−20.37	9.75	5.31

Table 6. Comparison of S_{11} result due to parametric variation of $T2$.

T2 (mm)	Frequency Band (GHz)	Maximum Reflection Coefficient (dB)	Resonant Frequency (GHz)	Bandwidth (GHz)
T2 = 3	2.19–2.69	−30.45	2.44	0.5
	4.06–6.62	−16.81	4.38	2.56
	8.02–10.00	−15.00	10.00	1.98
T2 = 4 (Proposed)	2.19–2.94	−19.18	2.5	0.75
	4.06–10.00	−26.53	4.31	5.94
T2 = 5	2.25–3.01	−19.15	2.5	0.76
	4.13–7.44	−25.34	4.38	3.31

parametric changes in side corner of the triangle are done to justify the better result. In Figure 8, three different values are shown. A comparison of S_{11} results is listed in Table 6.

3.3.4. Parametric Change in $T1$

The parametric change in the tapered cut at the right side corner of the patch is shown in Figure 9. From the patch, one small triangle from the right side of the corner is removed, and then the length of $T1$ is varied to get the best results. Three values are shown in Figure 9. The comparison of S_{11} results is listed in Table 7.

Table 7. Comparison of S_{11} results due to parametric variation of $T1$.

T1 (mm)	Frequency Band (GHz)	Maximum Reflection Coefficient (dB)	Resonant Frequency (GHz)	Bandwidth (GHz)
T1 = 2	2.19–2.94	−18.62	2.44	0.75
	4.13–10	−22.58	4.31	5.87
T1 = 3	2.19–2.96	−19.18	2.50	0.77
	4.06–10.00	−26.53	4.31	5.94
T1 = 4	2.25–3.01	−20.94	2.5	0.76
	4.13–10	−24.46	4.38	5.87

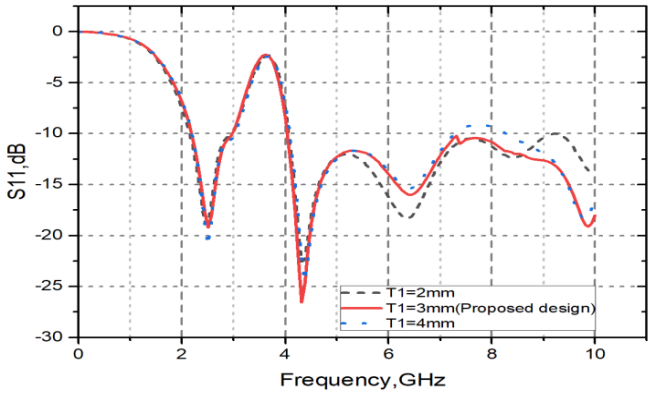

Figure 9. Simulation results of parametric change in $T1$.

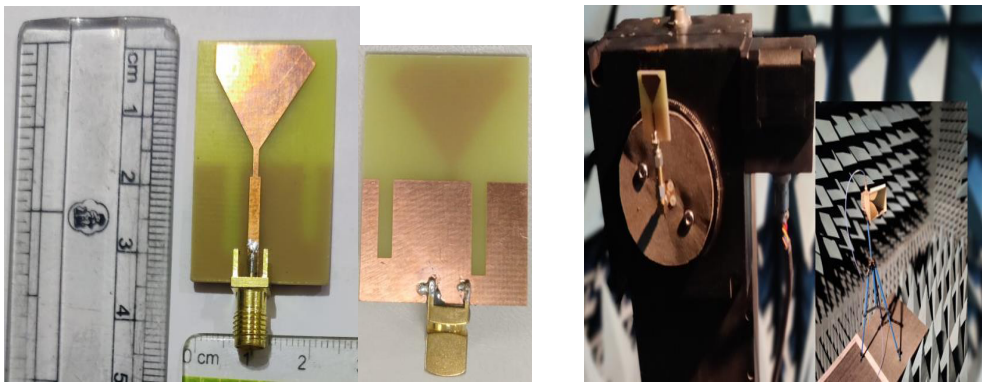

(a) (b)

Figure 10. Fabricated structure of the proposed antenna, (a) front side and back side, (b) testing of antenna at anechoic chamber.

4. EXPERIMENTAL RESULTS & DISCUSSION

After the complete analysis of all parametric variations, the structure is finalized and fabricated.

The fabricated proposed design is shown in Figure 10. In Figure 10(a), front side and backside of the proposed design are shown. In Figure 10(b), the testing of the proposed design is shown in an anechoic chamber. As already discussed, the proposed antenna is designed on an FR4 substrate and has partial ground plane. Antenna fabrication is done after simulating it through High-Frequency Structure Simulator (HFSS) software.

The comparative analysis of the simulated results and measured results is shown in Figure 11 for S_{11}, axial ratio, and gain. In all the results, there is a slight variation between the experimental and simulated results, due to the soldering and soldering temperature at the feedline. In Figure 11(a), the return loss graph is shown, while in Figures 11(b) and 11(c), plots of the axial ratio and gain graph respectively are shown. Table 8 shows the comparison of the return loss for the simulated and measured results. The proposed structure provides an impedance bandwidth of 6.88 GHz (0.89 GHz for the lower band and 5.99 GHz for the higher band). It is also observed that the proposed antenna has a moderate peak gain of 3.66 dB at 5.25 GHz. Table 9 gives a clear idea about the applications, which the proposed antenna can be used for.

Based on the final dimensions, the radiation pattern is plotted at each resonant frequency. Figure 12 shows the radiation pattern graph of the co-polarization and cross-polarization in E-plane and H-plane. At 4.31 GHz and 6.75 GHz, E-plane patterns are dipole in nature, but H-plane is omnidirectional which

Table 8. Comparison of the return loss between the simulated and measured value.

Reading	Frequency band (GHz)	Resonant Frequency (GHz)	Maximum Return loss (dB)	Bandwidth (GHz)
Measured	2.13–3.02 4.01–10.00	2.40 4.31 6.75 9.80	−25.18 −29.54 −22.95 −21.80	6.88
Simulated	2.19–2.94 4.06–10.00	2.50 4.3 6.44 9.87	−19.18 −26.54 16.01 −19.13	6.69

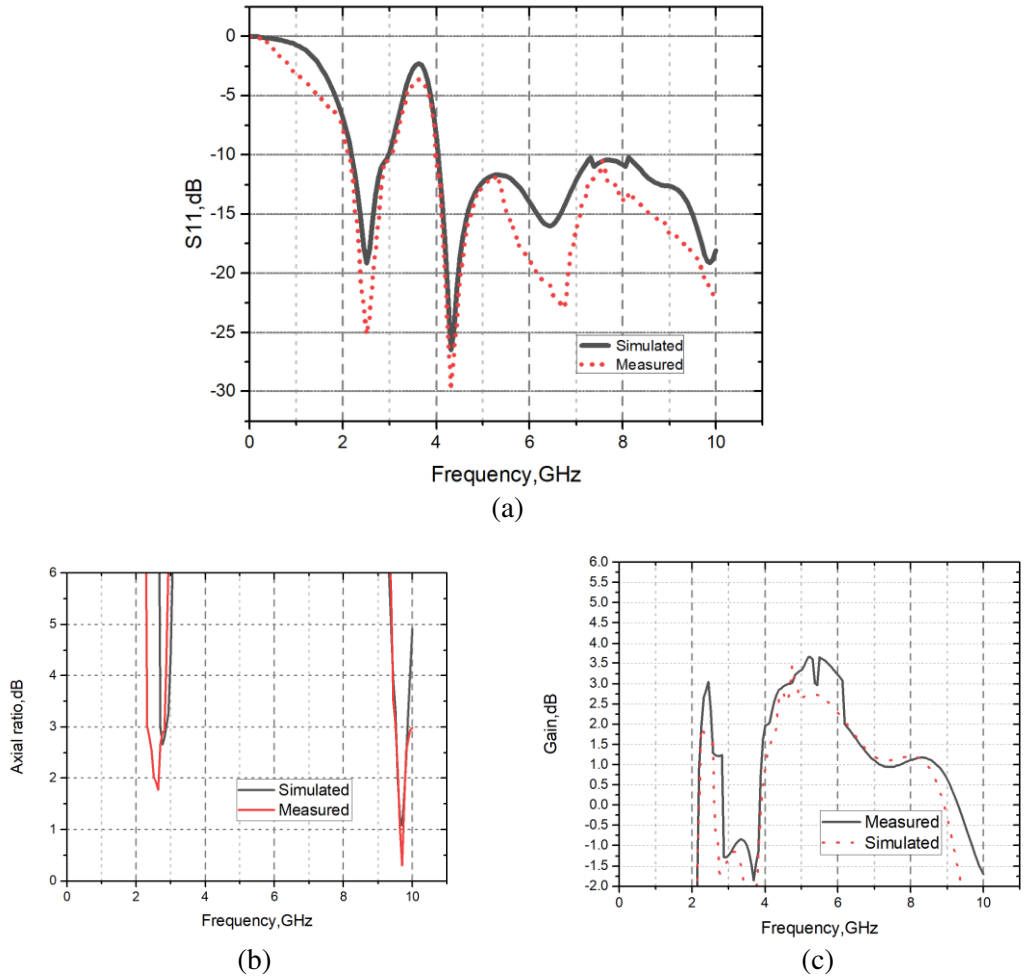

Figure 11. Simulated and measured results of proposed design, (a) return loss, (b) axial ratio, (c) gain.

is quite obvious in linear polarization. It is also observed that circular polarization is achieved at 2.4 GHz and 9.8 GHz, and hence directivity is less as seen in Figures 12(a) and 12(d) as the pattern is distorted omnidirectional. In Figures 12(b) and 12(c), directivity is high as the antenna is linearly polarized.

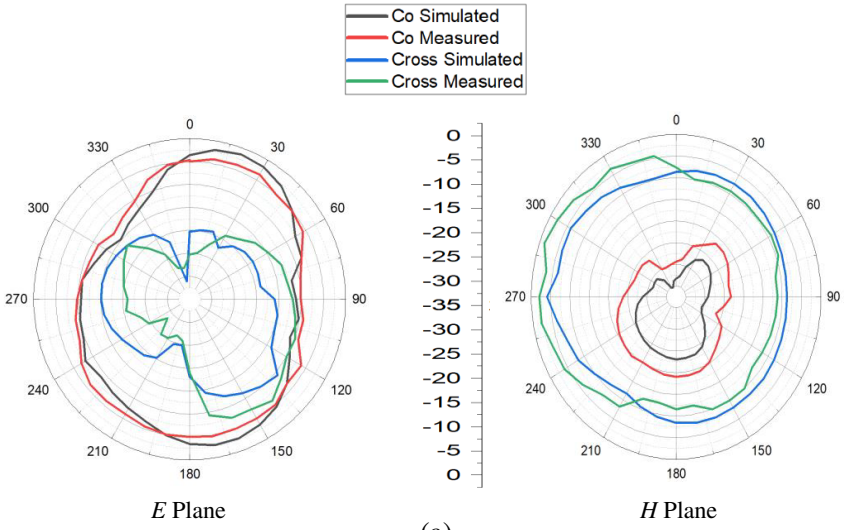

E Plane *H* Plane

(a)

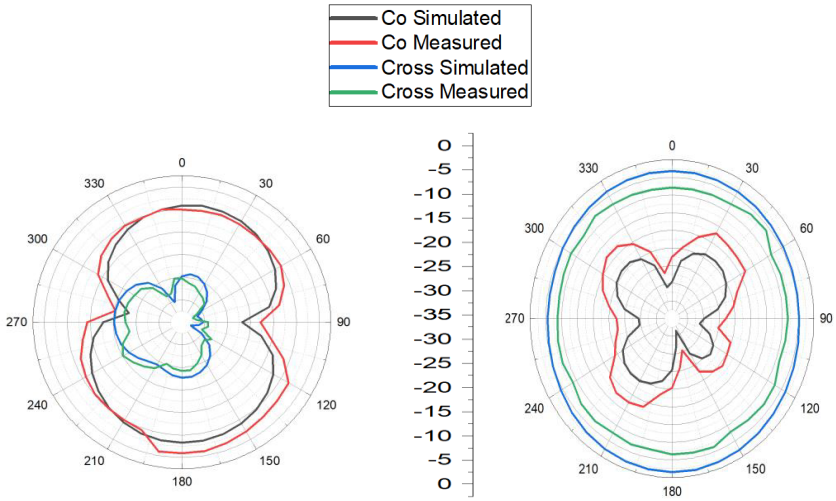

E Plane *H* Plane

(b)

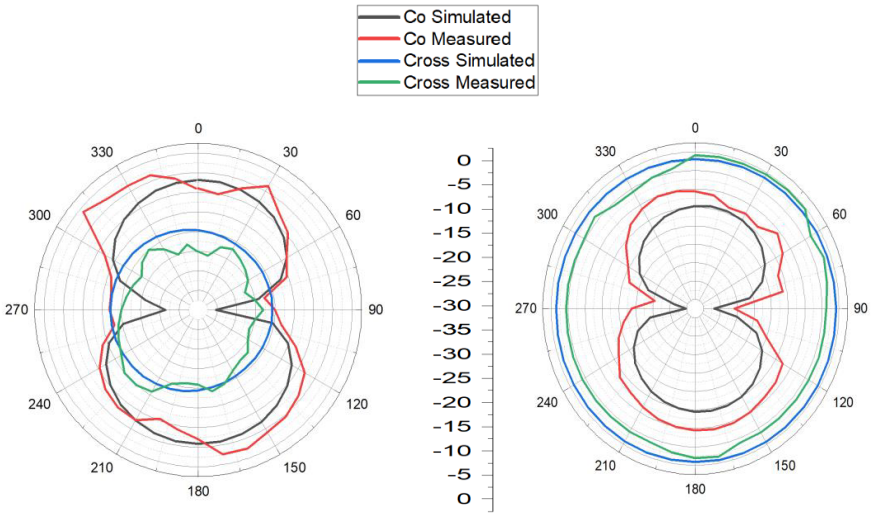

E Plane *H* Plane

(c)

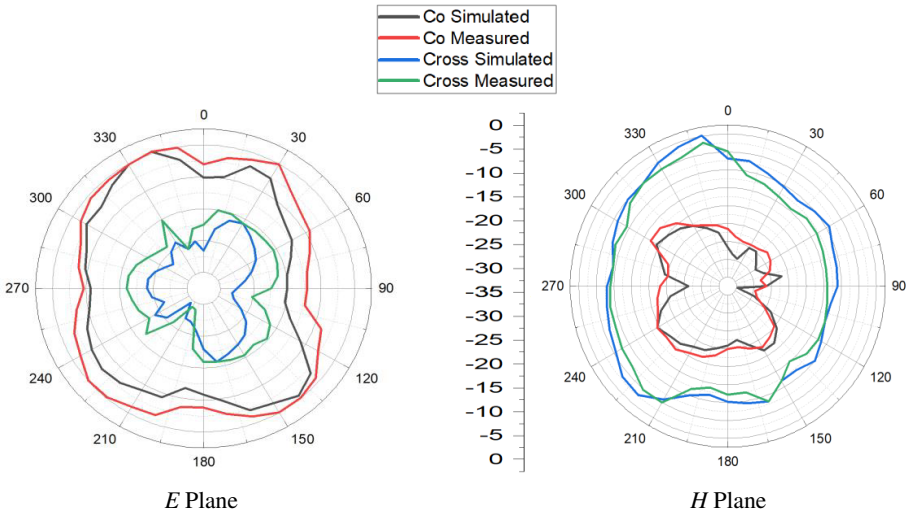

(d)

Figure 12. Simulated and measured radiation pattern graph at (a) 2.4 GHz, (b) 4.31 GHz, (c) 6.75 GHz, (d) 9.8 GHz.

Table 9. Frequency achieved from proposed design with its applications.

Measured Frequency	Application
2.4 GHz	RFID
4.31 GHz	Wi-Max
6.75 GHz	C-Band
9.8 GHz	X-band

Table 10. Comparison of the proposed design with similar existing designs.

Reference	Size (mm^3)	Frequency Range (GHz)	Bandwidth (GHz)	LP/CP	Peak Gain (dB)
[1]	37 × 28 × 1.6	1.96–2.22 3.51–3.91 4.78–5.26	0.26 0.4 0.48	2.07 (LP) 3.73 (LP) 4.96 (LP)	5
[13]	50 × 35 × 1.6	1.68–2.04 3.05–4.1 7.62–8.42	0.36 1.05 0.8	7.2 (CP)	3.5
[14]	56 × 52 × 3.2	2.09–2.64	0.55	2.3&2.6 (CP)	4.54
[17]	50 × 60 × 0.8	1.66–2.62	0.96	2.4 (CP)	4.7
[19]	42.5 × 42.5 × 1.6	5.15–12.47	7.32	5.5 (CP)	4.5
[21]	32 × 32 × 1.6	3.48–5.86	2.38	5.3 (CP)	5.32
[29]	60 × 60 × 1.58	2.12–2.28	0.16	2.2&2.4 (CP)	5.34
Proposed work	**35 × 24 × 1.6**	2.13 to 3.02 4.01 to 10.00	0.89 5.99	2.4&9.8 (CP) 4.31&6.75 (LP)	3.66

At all the frequencies shown, the undesired cross-polarization components are weaker in strength than co-polar components which are quite desirable.

From the radiation pattern, it is clear that antenna is linearly polarized at 4.31 and 6.75 GHz frequency, and it is circularly polarized at 2.4 and 9.8 GHz frequency. The measured axial ratio is shown at 2.32 to 2.81 GHz and 9.50 to 10.00 GHz bandwidths while simulated axial ratio is shown at 2.69 to 2.88 GHz and 9.56 to 9.81 GHz.

Moreover, the proposed antenna provides a higher bandwidth (although it yields a moderate value of gain) than most of the similar existing antennas shown in Table 10.

5. CONCLUSION

In this paper, a triangle-shaped multi-band antenna is presented. The antenna achieved linear polarization at frequencies 4.31 GHz (Wi-Max application) and 6.75 GHz (C-band application) and is circularly polarized at frequencies 2.4 GHz (RFID application) and 9.8 GHz (X-band application). The impedance bandwidth range is quite large 2.13 to 3.02 GHz and 4.01 to 10.00 GHz. The gain of the compact antenna is also quite acceptable (3.66 dB). The antenna is well suitable for Wi-Max, C-band, and X-band applications. This antenna is also suitable for vehicular communications and for portable wireless devices.

REFERENCES

1. Nallapaneni, S. and P. Muthusamy, "Design of multiband fractal antenna loaded with parasitic elements for gain enhancement," *International Journal of RF and Microwave Computer-Aided Engineering*, Vol. 31, No. 6, 2021, https://doi.org/10.1002/mmce.22622.
2. Malathy, E. M., V. Thanikachalam, and D. Ruby, "Metamaterial-loaded multiband antenna for embedded automotive internet-of-things communications," *International Journal of Communication Systems*, Vol. 34, No. 15, 2021, https://doi.org/10.1002/dac.4941.
3. Dey, A. B., D. Mitra, and W. Arif, "Design of CPW fed multiband antenna for wearable wireless body area network applications," *International Journal of RF and Microwave Computer-Aided Engineering*, Vol. 30, No. 12, 2020, https://doi.org/10.1002/mmce.22459.
4. Puri, S. C., S. Das, and M. G. Tiary, "A multiband antenna using plus-shaped fractal-like elements and stepped ground plane," *International Journal of RF and Microwave Computer-Aided Engineering*, Vol. 30, No. 5, 2020, https://doi.org/10.1002/mmce.22169.
5. Ali, T., K. D. Prasad, and R. C. Biradar, "A miniaturized slotted multiband antenna for wireless applications," *Journal of Computational Electronics*, Vol. 17, No. 3, 1056–1070, 2018, https://doi.org/10.1007/s10825-018-1183-z.
6. Anand, R. and P. Chawla, "Optimization of inscribed hexagonal fractal slotted microstrip antenna using modified lightning attachment procedure optimization," *International Journal of Microwave and Wireless Technologies*, Vol. 12, No. 6, 519–530, 2020, https://doi.org/10.1017/s1759078720000148.
7. Midya, M., S. Bhattacharjee, and M. Mitra, "Compact CPW-fed circularly polarized antenna for WLAN application," *Progress In Electromagnetics Research M*, Vol. 67, 65–73, 2018.
8. Gao, S. S., Q. Luo, and F. Zhu, *Circularly Polarized Antennas*, John Wiley & Sons, 2013.
9. Falade, O. P., M. Ur-Rehman, X. Yang, G. A. Safdar, C. G. Parini, and X. Chen, "Design of a compact multiband circularly polarized antenna for global navigation satellite systems and 5G/B5G applications," *International Journal of RF and Microwave Computer-Aided Engineering*, Vol. 30, No. 6, 2020, https://doi.org/10.1002/mmce.22182.
10. Iwasaki, H., "A circularly polarized small-size microstrip antenna with a cross slot," *IEEE Transactions on Antennas and Propagation*, Vol. 44, No. 10, 1399–1401, 1996, https://doi.org/10.1109/8.537335.

11. Nasimuddin, X. Qing, and Z. N. Chen, "A compact circularly polarized slotted patch antenna for GNSS applications," *IEEE Transactions on Antennas and Propagation*, Vol. 62, No. 12, 6506–6509, 2014, https://doi.org/10.1109/tap.2014.2360218.
12. Randy, O. T., Nasimuddin, and A. Alphones, "Circularly polarized slotted-ground microstrip antennas for radiofrequency identification readers," *Microwave and Optical Technology Letters*, Vol. 54, No. 10, 2304–2309, 2012, https://doi.org/10.1002/mop.27075.
13. Bag, B., P. Biswas, R. Mondal, S. Biswas, and P. P. Sarkar, "Circularly polarized quad-band monopole antenna of wireless communication system," *International Journal of RF and Microwave Computer-Aided Engineering*, Vol. 29, No. 9, 2019, https://doi.org/10.1002/mmce.21818.
14. Shaw, M., N. Mandal, and M. Gangopadhyay, "A compact circularly polarized isosceles triangular microstrip patch antenna with parasitic elements for multiband application," *Microwave and Optical Technology Letters*, Vol. 62, No. 10, 3275–3282, 2020, https://doi.org/10.1002/mop.32445.
15. Sharma, P. and K. Gupta, "Analysis and optimized design of single feed circularly polarized microstrip antennas," *IEEE Transactions on Antennas and Propagation*, Vol. 31, No. 6, 949–955, 1983, https://doi.org/10.1109/tap.1983.1143162.
16. Bairami, P., M. Fakheri, V. Rafii, and L. Asadpor, "Circularly polarized multi segment circular fractal array antenna by modified feed network for C-band application," *IETE Journal of Research*, Vol. 63, No. 2, 188–193, 2016, https://doi.org/10.1080/03772063.2016.1255157.
17. Sim, C. Y., W. C. Weng, M. H. Chang, and B. Y. Chen, "Annular-ring slot antenna designs with circular polarization radiation," *International Journal of RF and Microwave Computer-Aided Engineering*, Vol. 25, No. 4, 337–345, 2014, https://doi.org/10.1002/mmce.20867.
18. Dhara, R., S. K. Jana, and M. Mitra, "Tri-band circularly polarized monopole antenna for wireless communication application," *Radioelectronics and Communications Systems*, Vol. 63, No. 4, 213–222, 2020, https://doi.org/10.3103/s0735272720040044.
19. Verma, M. K., B. K. Kanaujia, J. P. Saini, and P. Singh, "A compact multi-slots loaded gap coupled CP antenna with DGS for WLAN/WiMAX applications," *International Journal of RF and Microwave Computer-Aided Engineering*, Vol. 30, No. 12, 2020, https://doi.org/10.1002/mmce.22431.
20. Khandelwal, M. K., S. Kumar, and B. K. Kanaujia, "Design, modeling and analysis of dual-feed defected ground microstrip patch antenna with wide axial ratio bandwidth," *Journal of Computational Electronics*, Vol. 17, No. 3, 1019–1028, 2018, https://doi.org/10.1007/s10825-018-1173-1.
21. Srivastava, K., B. Mishra, and R. Singh, "Microstrip-line-fed inverted L-shaped circularly polarized antenna for C-band applications," *International Journal of Microwave and Wireless Technologies*, Vol. 14, No. 4, 502–510, 2021, https://doi.org/10.1017/s1759078721000635.
22. Tharehalli Rajanna, P. K., K. Rudramuni, and K. Kandasamy, "Compact triband circularly polarized planar slot antenna loaded with split ring resonators," *International Journal of RF and Microwave Computer-Aided Engineering*, Vol. 29, No. 12, 2019, https://doi.org/10.1002/mmce.21953.
23. Le, T. T., H. H. Tran, and T. K. Nguyen, "Compact broadband circularly polarized slot-patch antenna array," *International Journal of RF and Microwave Computer-Aided Engineering*, Vol. 29, No. 1, e21468, 2018, https://doi.org/10.1002/mmce.21468.
24. Alam, M., Mainuddin, B. Kanaujia, M. Beg, S. Kumar, and K. Rambabu, "A hexa-band dual-sense circularly polarized antenna for WLAN/Wi-MAX/SDARS and C-band applications," *International Journal of RF and Microwave Computer-Aided Engineering*, Vol. 29, No. 4, e21599, 2018, https://doi.org/10.1002/mmce.21599.
25. Sung, Y., "Circularly polarized patch antenna with two different C-shaped ring structures," *Microwave and Optical Technology Letters*, Vol. 61, No. 12, 2773–2780, 2019, https://doi.org/10.1002/mop.31972.
26. Lu, J.-H. and K.-L. Wong, "Single-feed circularly polarized equilateral-triangular microstrip antenna with a tuning stub," *IEEE Transactions on Antennas and Propagation*, Vol. 48, No. 12, 1869–1872, 2000, https://doi.org/10.1109/8.901278.

27. Ding, K., T. Yu, D.-X. Qu, and C. Peng, "A novel loop-like monopole antenna with dual-band circular polarization," *Progress In Electromagnetics Research C*, Vol. 45, 179–190, 2013.
28. Srivastava, K., B. Mishra, A. K. Patel, and R. Singh, "Circularly polarized defected ground stub-matched triple-band microstrip antenna for C- and X-band applications," *Microwave and Optical Technology Letters*, Vol. 62, No. 10, 3301–3309, 2020, https://doi.org/10.1002/mop.32450.
29. Shinde, J. P., R. Kumar, and M. D. Uplane, "Circular polarization in defected hexagonal-shaped microstrip antenna," *Wireless Personal Communications*, Vol. 75, No. 2, 843–856, 2013, https://doi.org/10.1007/s11277-013-1394-3.
30. Mishra, B., V. Singh, and R. Singh, "Dual and wide-band slot-loaded stacked microstrip patch antenna for WLAN/WiMAX applications," *Microsystem Technologies*, Vol. 23, No. 8, 3467–3475, 2016, https://doi.org/10.1007/s00542-016-3120-z.